

# Mechanism of Hairpin-Duplex Conversion for the HIV-1 Dimerization Initiation Site\*<sup>§</sup>

Received for publication, March 23, 2005, and in revised form, August 19, 2005 Published, JBC Papers in Press, September 15, 2005, DOI 10.1074/jbc.M503230200

Serena Bernacchi<sup>‡1,2</sup>, Eric Ennifar<sup>§1</sup>, Katalin Tóth<sup>‡</sup>, Philippe Walter<sup>§</sup>, Jörg Langowski<sup>‡</sup>, and Philippe Dumas<sup>§3</sup>

From the <sup>§</sup>Institut de Biologie Moléculaire et Cellulaire, UPR 9002 du CNRS Conventionnée à l'Université Louis Pasteur Strasbourg, 15 Rue René Descartes, F-67084 Strasbourg Cedex, France and <sup>‡</sup>German Cancer Research Center, Division of Biophysics of Macromolecules, Im Neuenheimer Feld 580, D-69120 Heidelberg, Germany

We have used the dimerization initiation site of HIV-1 genomic RNA as a model to investigate hairpin-duplex interconversion with a combination of fluorescence, UV melting, gel electrophoresis, and x-ray crystallographic techniques. Fluorescence studies with molecular beacons and crystallization experiments with 23-nucleotide dimerization initiation site fragments showed that the ratio of hairpin to duplex formed after annealing in water essentially depends on RNA concentration and not on cooling kinetics. With natural sequences allowing to form the most stable duplex, and thus also the loop-loop complex (or “kissing complex”), concentrations as low as 3  $\mu\text{M}$  in strands are necessary to obtain a majority of the hairpin form. With a mutated sequence preventing kissing complex formation, a majority of hairpins was even obtained at 80  $\mu\text{M}$  in strands. However, this did not prevent an efficient conversion from hairpin to duplex in the presence of salts. Kinetic considerations are in favor of duplex formation from intermediates involving hairpins engaged in cruciform dimers rather than from free strands. The very first step of formation of such a cruciform intermediate could be trapped in a crystal structure. This mechanism might be significant for the dynamics of small RNAs beyond the strict field of HIV-1.

Stem-loops and bulged loops are common motifs found in RNA secondary structure and are often involved in RNA-protein or RNA-RNA recognition. Because of the self-complementarity of stems, a stem-loop structure can also adopt an alternative duplex structure containing unpaired nucleotides. This hairpin-duplex equilibrium also represents a major problem in structural studies of nucleic acids by NMR and x-ray crystallography, both requiring concentrated samples. Strategies using a mixture of unlabeled and <sup>15</sup>N-labeled oligonucleotides were developed to discriminate between the two species by NMR (1, 2). However, many attempts at crystallizing RNA or DNA stem-loop structures led unexpectedly to duplex crystal structures (3–6). This was even the case for the unusually stable RNA tetraloops belonging to the GNRA, UNCG, and CUUG families, which are supposed to be nucleation points for RNA folding because of their stability and quick folding kinetics (see “Discussion” in Ref. 7). Significantly, this problem does not seem to spread to NMR studies because several RNA stem-loop structures were successfully solved by using this technique, whereas most of the hairpin

structures described by x-ray crystallography were obtained from complexes with proteins (8–10) or were embedded in a larger RNA context, as for tRNAs, hammerhead ribozyme, and ribosome structures. The only notable exception is the GAGA tetraloop found in the sarcin-ricin loop, successfully crystallized as a hairpin (11, 12).

The present study focuses on the dimerization initiation site (DIS)<sup>4</sup> of HIV-1 genomic RNA that has been extensively studied by several biochemical and biophysical methods. This strongly conserved stem-loop sequence (13) (Fig. 1a) was shown to be crucial for viral RNA dimerization and packaging, two major determinants of viral infectivity (14, 15). The DIS loop is made of nine nucleotides, six of them being self-complementary. This allows the DIS to initiate RNA dimerization through loop-loop interaction and formation of a “kissing complex” (for a review see Ref. 16) (Fig. 1b). Among all natural HIV-1 isolates, only two self-complementary sequences are commonly found, AGGUGCACA and AAGCGCGCA, representative of HIV-1 subtypes A and B, respectively (13). Alternatively, the DIS can dimerize as a duplex form through extension of intermolecular base pairing of the kissing complex (Fig. 1b). This extended duplex is associated with the stabilization of the dimer observed *in vitro* upon heat treatment at 55 °C or by the addition of the viral nucleocapsid protein NCp7 (17).

Here we use a 23-nucleotide fragment of the HIV-1 DIS as a model to address the question of the dynamics of hairpin-duplex interconversion for short self-complementary RNA sequences. The present work started with our first attempts at crystallizing the kissing complex form of the DIS, which led to the crystallization of the duplex form (18, 19) as frequently observed for other RNA hairpin structures. As usually done, we were relying on a “flash cooling” of the RNA sample to freeze the RNA molecules into their hairpin conformation and prevent duplex formation. This remained unsuccessful. We finally obtained kissing complex crystals (20), but only after sufficient lowering of the RNA concentrations during the annealing procedure, which was an obvious indicator of a strong duplex-forming propensity. It thus became evident that a direct method of investigation was necessary to delineate a “cooling time-RNA concentration” phase diagram. The hairpin-duplex equilibrium for the DIS(Mal) and DIS(Lai) wild-type sequences, representative of HIV-1 subtypes A and B, was investigated by labeling both sequences at their 3' and 5' extremities with a dye and a fluorescence quencher, respectively, thus forming a molecular beacon (21). Such a labeled sequence, when mixed with the excess of an unlabeled sequence, allows us to distinguish unambiguously the DIS hairpin within the kissing complex, from the duplex form (Fig. 2).

We also reinvestigated hairpin-duplex interconversion for the HIV-1

\* This work was supported by the Agence Nationale de Recherche sur le SIDA. The costs of publication of this article were defrayed in part by the payment of page charges. This article must therefore be hereby marked “advertisement” in accordance with 18 U.S.C. Section 1734 solely to indicate this fact.

<sup>§</sup> The on-line version of this article (available at <http://www.jbc.org>) contains Figs. S1–S4.

<sup>1</sup> Both authors contributed equally to this work.

<sup>2</sup> A German Cancer Research Center (Deutsches KrebsForschungsZentrum) fellow.

<sup>3</sup> To whom correspondence should be addressed. Tel.: 33-388-417-002; Fax: 33-388-602-218; E-mail: p.dumas@ibmc.u-strasbg.fr.

<sup>4</sup> The abbreviations used are: DIS, dimerization initiation site; HIV, human immunodeficiency virus; NCp7, nucleocapsid protein (7 kDa); MES, 4-morpholineethanesulfonic acid; FAM, 5 (and 6)-carboxyfluorescein; Pur, purine; TAR, *trans*-activation response element; cTAR, complementary TAR.

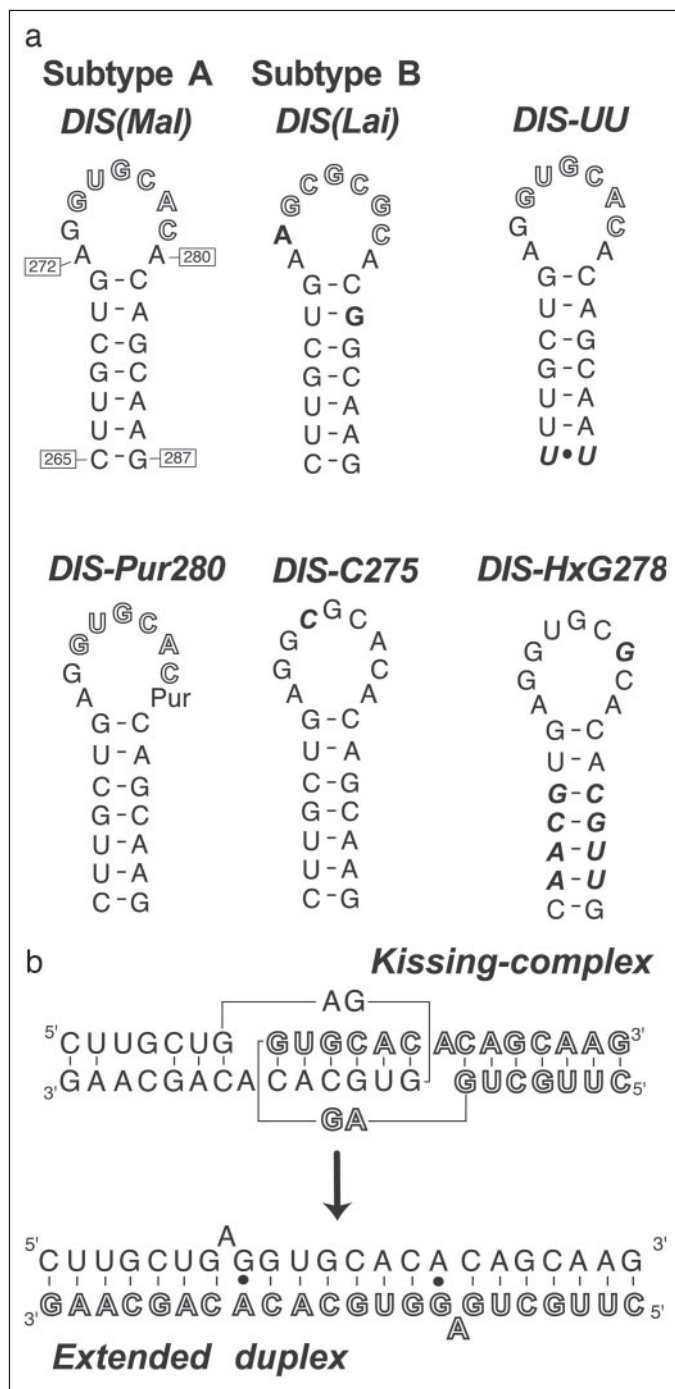


FIGURE 1. The HIV-1 DIS. *a*, sequence and secondary structure of wild-type and mutant DIS stem-loops used in this study. *b*, secondary structure of the kissing complex and the extended duplex formed upon DIS dimerization.

DIS by UV-melting studies. This led us to point a subtle difference between the DIS(Mal) and DIS(Lai) sequences because of close duplex and hairpin melting temperatures. Finally, we showed that the formation of a stable kissing complex is not necessary to convert significantly a hairpin form into a duplex at low temperature. Instead, with a loop sequence preventing kissing complex formation, we found that duplex formation can only be explained by hairpins forming cruciform intermediates, and not by their full melting prior to strand re-association. Possible biological implications of this process in the HIV-1 life cycle, and beyond the strict field of HIV-1, are discussed.

## MATERIALS AND METHODS

**RNA Synthesis and Purification**—DIS(Mal) and DIS(Lai) sequences doubly labeled as molecular beacons were chemically synthesized in our laboratory on a 392 DNA/RNA synthesizer (Applied Biosystems, Foster City, CA) with synthons from Eurogentec (Seraing, Belgium). Labeling of the 5' terminus with 5 (and 6)-carboxyfluorescein (FAM) was performed via an amino-linker with a six-carbon spacer arm. The 3' terminus was labeled with a universal fluorescence quencher, the 4-(4'-dimethylethylaminophenylazo)benzoic acid. Unlabeled and 5'-FAM singly labeled RNA sequences were purchased from Dharmacon (Boulder, CO). The unlabeled sequences correspond to the natural DIS(Mal) and DIS(Lai) sequences and to the mutated sequences DIS-UU, DIS-Pur280, DIS-C275, and DIS-HxG278 (Fig. 1*a*). The DIS-UU, containing an unstable U-U mismatch at the beginning of the stem, was designed for previous crystallization studies of the loop-loop complex (20). The RNAs were purified as described previously (19).

**Sample Preparation**—Oligonucleotide concentrations (expressed in strands) were derived from extinction coefficients at 260 nm of 223,200  $M^{-1} cm^{-1}$  for DIS(Mal), 216,400  $M^{-1} cm^{-1}$  for DIS(Lai), 220,100  $M^{-1} cm^{-1}$  for DIS-C275, 225,100  $M^{-1} cm^{-1}$  for DIS-HxG278, and 224,600  $M^{-1} cm^{-1}$  for DIS-UU. RNA folding was achieved by diluting the samples in 200  $\mu l$  of water in an Eppendorf tube at different concentrations (0.6, 6, and 60  $\mu M$ ), heating at 90  $^{\circ}C$  for 3 min, and then cooling to 0  $^{\circ}C$  with three different kinetics. The two fast cooling kinetics were monitored with a thermocouple plugged to a data acquisition module OMB-DAQ-55 (Omega Engineering Inc., Stamford, CT). First, slow cooling was achieved by imposing a linear decrease of temperature for 3 h. Second, a so-called "fast cooling" was achieved in melting ice, which results in a rather slow exponential decrease of temperature with a half-time between 10 and 19 s depending on the position of the thermocouple between the wall and the center of the Eppendorf tube. Finally, a supposedly "ultra-fast cooling" was achieved in ethanol maintained at  $-70^{\circ}C$  with dry ice. This results in cooling with an average half-time of 5 s, until a plateau is reached at 0  $^{\circ}C$  and maintained during a few seconds because of ice formation. Notably, 16–18 s are still necessary to go from 90 to 0  $^{\circ}C$  with the latter method.

**Optical Measurements**—Fluorescence emission spectra were recorded at  $20.0 \pm (0.5)^{\circ}C$  on an SLM-Aminco 8100 spectrofluorimeter (SLM, Urbana, IL) using a 150-watt xenon lamp. The excitation and emission bandwidths were 8 nm. Steady-state fluorescence measurements were performed by mixing a fixed concentration of DIS molecular beacon (60 nM) with an excess of nonlabeled RNA. The nonlabeled RNA to molecular beacon ratios ranged from 10 to 1000, corresponding to a total RNA concentration ranging from 600 nM to 60  $\mu M$ . Samples were folded as described above, and measurements were achieved in water to probe the result of the folding in the absence of salt and buffer. The fluorescence signal was found stable and reproducible in such conditions. To evaluate the influence of the excess of nonlabeled RNA on the fluorescence of the FAM dye, experiments were repeated by using a singly labeled DIS-5'-FAM. For each value of the ratio, the relative increase of fluorescence ( $R$ ) was calculated. To determine the percentage of extended duplex forms in solution,  $R$  values were then compared with the increase of fluorescence relative to the singly labeled DIS-5'-FAM, which corresponds to the full fluorescence restoration that can be obtained by this system.

Absorption spectra were recorded either on a Cary 4E (Varian, Sydney, Australia) or with a Uvikon XL (SECOMAM, Domont, France) spectrophotometer equipped with a Peltier thermostated cell holder. Melting curves were recorded at 260 nm with a heating rate of  $0.25^{\circ}C \cdot min^{-1}$  between 10 and 85  $^{\circ}C$ . The temperature was measured by

## Hairpin-Duplex Conversion

a thermocouple inserted into one cell. 20 mM sodium cacodylate, pH 6.5, 25 mM potassium acetate, 2 mM magnesium acetate were used as buffer.

**Melting Curve Processing**—The UV melting curves were processed within the frame of the usual two-state approximation (22). However, we derived the melting temperature ( $T_m$ ) and variation of enthalpy  $\Delta H$  by using a method slightly different from the usual one.<sup>5</sup> The DIS(Mal) showed a concentration-independent hairpin melting at high temperature and could be analyzed following this method. For the DIS(Lai), however, the situation was more complicated and a detailed analysis, based upon numerical integration of the set of differential equations describing the different equilibria, was necessary to explain the observations.<sup>5</sup>

**Gel Electrophoresis Experiments and Quantification**—DIS-C275 RNA samples were prepared (at concentrations of 20, 9, 4.5, and 2.2  $\mu\text{M}$ ) as described above and analyzed on 15 or 20% native PAGE performed at 4 °C in TBM buffer (45 mM Tris borate, pH 8.3, 1 mM  $\text{MgCl}_2$ ). Hairpin and duplex quantification was performed on a Gel Doc 1000 (Bio-Rad) after ethidium bromide (EtBr) staining of the gel after electrophoresis. Because a dimeric duplex probably retains more than twice the amount of ethidium bromide retained by a monomeric hairpin, we used a ratio of 2.5. The data obtained in such a way yielded  $\sim 10\%$  of the duplex form after annealing in water, in good agreement with 12% from fluorescence measurement. For the sake of comparison, the experiment on the effect of magnesium concentration at 2  $\mu\text{M}$  RNA was quantified by <sup>32</sup>P labeling. The RNAs were 5'-end-labeled for 30 min at 37 °C with [ $\gamma$ -<sup>32</sup>P]ATP (Amersham Biosciences) and T4 polynucleotide kinase. Radioactivity was measured on a BAS 2000 Bio-Imager (Fuji). The quantification was performed with a specific program written with Mathematica (Wolfram Research).

**RNA Crystallization**—For kissing complex crystallization, RNA samples were diluted in water to 6  $\mu\text{M}$  or less, annealed at 90 °C, and either submitted to the fast cooling protocol or slowly cooled to room temperature. A low salt dimerization buffer (8 mM  $\text{MgCl}_2$ , 30 mM sodium cacodylate, pH 7.0) was added prior to incubation at 37 °C for 1 h (however, further refinement of the crystallization protocol showed that this dimerization step was not required), and samples were concentrated to 360–600  $\mu\text{M}$ . Drops were made by mixing 3  $\mu\text{l}$  of RNA sample with 3  $\mu\text{l}$  of a well solution (100 mM ammonium sulfate, 50 mM MES, pH 5.6, 20% PEG 8000, 10 mM  $\text{MgCl}_2$ ) and 2  $\mu\text{l}$  of a 3 mM spermine solution. Single platelet crystals (up to 0.8 mm in size) belonging to the space group C22<sub>1</sub> were obtained after 2–3 days of equilibration by vapor diffusion at 37 °C. Kissing complex crystals were also obtained with a mutated DIS(Mal) sequence, where the 1st bp of the stem was replaced by a U-U mismatch. This DIS-UU sequence was crystallized as a kissing complex in different conditions but by using a similar protocol. After annealing, the dimerization buffer (8 mM  $\text{MgCl}_2$ , 30 mM sodium cacodylate, and 7 mM spermine) was added. The sample was concentrated to 150  $\mu\text{M}$ , and drops were made by mixing 1 volume of RNA sample with 1 volume of well solution (20 mM  $\text{MgCl}_2$ , 50 mM MES, pH 6.0, 15% isopropyl alcohol). Large platelet crystals (up to 1 mm) of space group C2 were obtained at 20 °C within 2–4 days. DIS(Mal) duplex crystals were obtained as described previously in Ref. 19.

**Numerical Values**—The different kinetic and equilibrium “constants” were expressed as in Equations 1–3,

$$k_{\text{on}}(T) = k_0 e^{-\frac{E_a}{RT}} \quad (\text{Eq. 1})$$

$$k_{\text{off}}(T) = \frac{k_{\text{on}}(T)}{K(T)} \quad (\text{Eq. 2})$$

$$K(T) = e^{\frac{\Delta H}{R} \left( \frac{1}{T_m} - \frac{1}{T} \right)} \quad (\text{Eq. 3})$$

with  $R$  the gas constant (1.987 cal·mol<sup>-1</sup>·K<sup>-1</sup>; 1 cal = 4.184 J);  $T$  the absolute temperature;  $T_m$  the melting temperature ( $K$ );  $E_a$  the activation energy;  $\Delta H$  the variation of enthalpy (kcal·mol<sup>-1</sup>);  $k_0$  the pre-exponential factor (min<sup>-1</sup> for a unimolecular transition and M<sup>-1</sup> min<sup>-1</sup> for a bimolecular transition); and  $K(T)$  the equilibrium constant. In the following the kinetic and equilibrium constants for hairpin and duplex formation will be numbered 1 and 2, respectively.

For hairpin formation  $K_1(T)$  is dimensionless, and  $T_{m1}$  is concentration-independent, whereas for duplex formation  $K_2(T)$  has the dimension of M<sup>-1</sup> and  $T_{m2}$  is given for a standard concentration of 1 M in strands. For hairpin closing, the kinetic constant is almost temperature-independent with  $k_{\text{on}} \sim 10^5 \text{ s}^{-1}$  and  $k_{\text{off}} = k_{\text{on}}$  at  $T = T_{m1}$  (23). The activation energy  $E_{a1}$  of hairpin opening is close and at least equal to  $|\Delta H_1|$  involved in hairpin closing. For duplex formation, the kinetic constant  $k_0$  is of order  $10^6 \text{ M}^{-1} \text{ s}^{-1}$ , and the (apparent) activation energy  $E_{a2}$  may be negative because of duplex formation not being an elementary mechanism (24, 25). Values less than  $-5 \text{ kcal}\cdot\text{mol}^{-1}$  are possible.

## RESULTS

**Hairpin-Duplex Equilibrium**—Kissing complex and duplex forms cannot be easily quantified in solution by classical gel studies because both forms have the same overall shape and essentially the same base-pairing pattern (19, 20). Therefore, to assess the effect of cooling kinetics and RNA concentration, we used DIS sequences labeled as molecular beacons (21) (Fig. 2). By mixing such doubly labeled 23-mer DIS with an excess of unlabeled RNA, we quantified the relative amount of duplex and consequently the amount of hairpins (either free or in kissing complexes). We observed for “slow” and “fast cooling” that the hairpin is predominant at low RNA concentrations (less than 3  $\mu\text{M}$ ), whereas almost only duplex species are formed at 60  $\mu\text{M}$  (Fig. 3). Our results clearly show that in this DIS system, the RNA concentration, and not the kinetics of cooling, is by far the predominant parameter for obtaining the hairpin form after the folding procedure. More importantly, we reproducibly observed an important increase of fluorescence in a narrow RNA concentration range (from 3 to 6  $\mu\text{M}$ ) with the ultra-fast cooling procedure. At first glance this might indicate an unexpected increase of duplex formation under conditions that favor the hairpin form. In this case, however, the enhanced increase of fluorescence most likely results from kinetically trapped misfolded di- or multimeric species. Finally, to test whether the observed increase of fluorescence was indeed specifically because of duplex formation, an excess of DIS-HxG278 containing a stem sequence partly inverted and unable to heterodimerize with the wild-type DIS sequence (Fig. 1a) was mixed with a fixed amount of molecular beacon. As shown in Fig. 3, no significant increase of fluorescence is observed in such conditions, which is strong evidence that its increase with a wild-type DIS is not because of unspecific effects.

We also performed similar investigations with the DIS-C275 mutant of the DIS(Mal) (Fig. 1a) by using gel electrophoresis techniques. As described in Ref. 26, the C275 mutation in the loop on the DIS(Mal) sequence abolishes kissing complex formation by introducing two highly destabilizing A-C mismatches in the loop-loop helix. This mutant was thus very convenient to study the hairpin-duplex transition by using classical gel experiments as described in Ref. 27. The fraction of

<sup>5</sup> P. Dumas, S. Bernacchi, and E. Ennifar, manuscript in preparation.

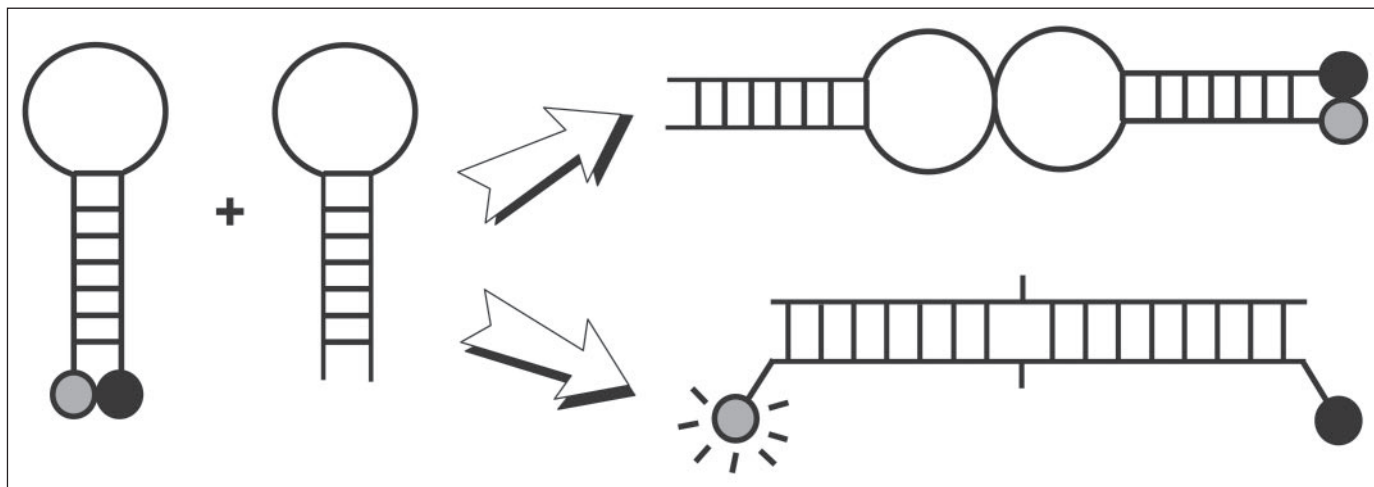


FIGURE 2. The molecular beacon strategy; a DIS stem-loop labeled 5' with a fluorescent dye and 3' with a fluorescence quencher is mixed with a large excess of unlabeled sequences. In the stem-loop structure (either as a monomeric form or involved in a kissing complex), both dyes are close to each other, and no fluorescence is observed. In the duplex form, the two dyes are far from each other, and fluorescence is restored.

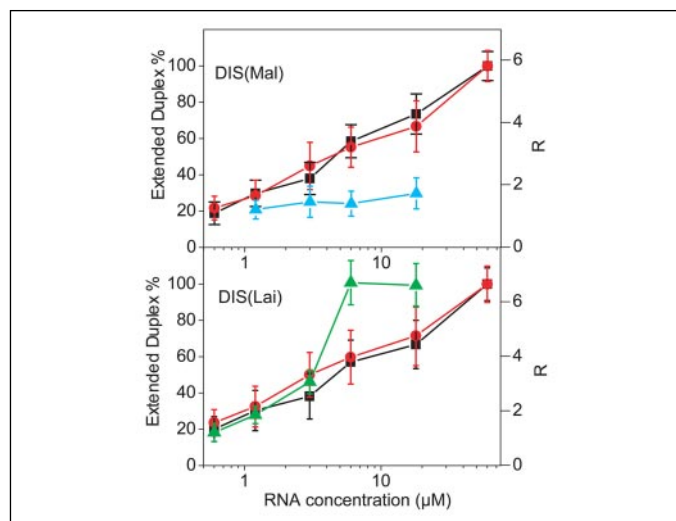


FIGURE 3. Fluorescence quantification of the relative amount of extended duplex formed in water after the folding procedure. The relative increase of fluorescence ( $R$  axis on the right) is converted in percentage of duplex on the left. Values obtained after flash cooling on ice (black squares) or slow cooling (red circles) are reported for the DIS(Mal) and DIS(Lai) sequences. Increase of fluorescence ( $R$  axis) obtained with an ultra-fast cooling at  $-70$  °C is reported as green triangles for the DIS(Lai) sequence. The increase of fluorescence measured in the presence of a fixed amount of DIS(Mal) doubly labeled molecular beacon, and of an excess of unlabeled DIS-HxG278 in different concentrations, is reported as blue triangles. This shows the sequence specificity of the fluorescence increase when an unlabeled wild-type DIS is used.

duplex was first evaluated in water, immediately after the cooling procedure, as a function of RNA concentration and of the kinetics of cooling. As observed with molecular beacons, our results on the gel emphasize the importance of the RNA concentration during RNA folding in comparison with a minor effect of the cooling process (Fig. 4). However, the hairpin fraction for the DIS-C275 mutant is much higher than for the wild-type sequence for all tested concentrations.

**Thermal Stability of the DIS Sequence**—We further investigated the kissing complex/duplex equilibrium by UV melting. A previous study made on the DIS(Lai) concluded that the kissing complex was converted into the duplex form at low temperature (around 25–30 °C), followed by a melting of the latter at 61 °C (28). The identification of the major peak of the differential melting curve as corresponding to duplex melting was based on the dependence of the melting temperature with concentration. However, on the basis of theoretical considerations and of a large

body of experimental results in the literature (for example see Refs. 29 and 30), we were led to question the fact that the DIS hairpin could melt at such a low temperature. In addition, our own results on the DIS(Mal) showed a concentration-independent peak at 72 °C (Fig. 5a) yielding an enthalpy value consistent with a 7-bp hairpin ( $|\Delta H_1| = 51.5 \text{ kcal}\cdot\text{mol}^{-1}$ ). Furthermore, by interpreting the high temperature peak for the DIS(Lai) as that of duplex melting not only led to poor fit of the experimental curves (not shown) but also to unacceptably low enthalpy values for a 20-bp duplex (around 60  $\text{kcal}\cdot\text{mol}^{-1}$ ). Finally, another clue was obtained by considering two DIS(Mal) mutants. The DIS-C275 mutant (Fig. 1a) unable to form a kissing complex, but not a hairpin, showed the same hairpin melting temperature and a significant modification at lower temperatures that can only be interpreted as duplex destabilization (Fig. 5b). In addition, the Pur280 mutant (Fig. 1a) obtained by the replacement of the A280 base by an adenine base deprived of its exocyclic amino group led to a significant modification of the melting profile (Fig. 5b), which is also because of duplex destabilization, whereas the peak characteristic of the hairpin at 72 °C remained unaffected. This fits perfectly with the DIS(Mal) duplex being affected by an A280Pur modification because A280 is engaged in a G-A “Watson-Crick-like” base pair in this duplex (19), and with the hairpin being unaffected by the same modification because A280 is unpaired in the kissing complex (20). Notably, the G-A mismatches contributing to duplex stability is well documented (31–33). This also indicated that, in the range of concentrations in use, the melting of the DIS(Mal) duplex occurs at a temperature close to and below that of the hairpin.

By comparison with the DIS(Mal), it was thus beyond any doubt that the major peak of the differential melting curve for the closely related DIS(Lai) was also a mark of the hairpin. However, as recalled above, this peak was concentration-dependent (28), which is in contradiction with a purely unimolecular transition. We finally clarified the situation by showing that the concentration dependence is because of almost simultaneous melting of the hairpin and of the duplex, and not to pure duplex melting. This was done by making use of numerical simulations that were confirmed by experiments.<sup>5</sup> This led to the conclusion that the subtle different behavior of the two sequences is because of the melting temperature of the DIS(Lai) duplex being close enough to that of the hairpin to cause an apparent concentration dependence of it, whereas the melting temperature of the DIS(Mal) duplex is sufficiently far from that of the hairpin to prevent any interference. The simulations also

## Hairpin-Duplex Conversion

**FIGURE 4. Comparison of hairpin fraction obtained with different RNA sequences after folding at different concentrations with slow cooling (solid lines) or fast cooling procedures (dotted lines).** The data for the DIS-C275 (open circles) were obtained from gel electrophoresis experiments, and the data for the DIS(Mal) (open triangles) are those from Fig. 3. The data for the DIS(Lai) were not reported for clarity because they overlap with those of the DIS(Mal). The other sequence data ( $\Delta$ C56,  $\Delta$ A58, and  $\Delta$ U59) are from Ref. 27 and were obtained from similar gel electrophoresis experiments. The sequences can be ranked in the order  $\Delta$ C56  $\ll$   $\Delta$ A58  $<$   $\Delta$ U59  $<$  DIS-(Mal,Lai) for their loop self-complementarity, which is also the order in which they appear along the curved arrow. This highlights the crucial importance of loop self-complementarity for the effect of RNA concentration on duplex formation, whereas the kinetics of cooling has comparatively a weak, or even null, importance.

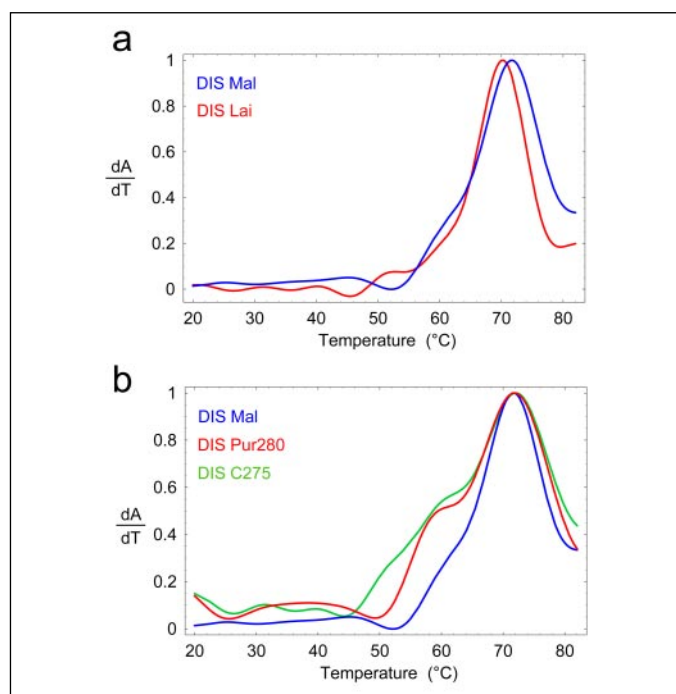
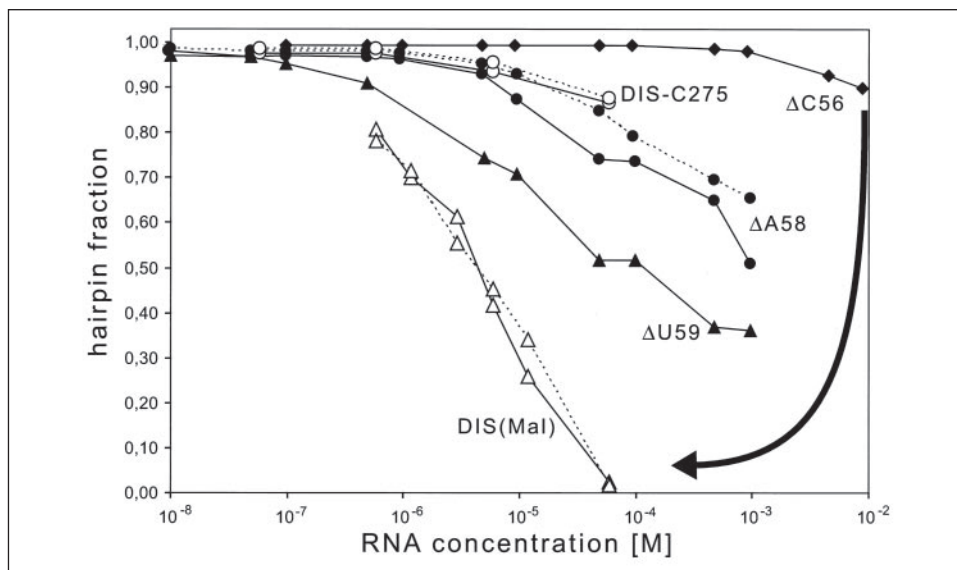


**FIGURE 5. Normalized derivative melting curves.** *a*, comparison of the natural DIS(Mal) and DIS(Lai) sequences. Note the sharper peak for the DIS(Lai) because of almost simultaneous melting of the duplex (see text). *b*, comparison of the natural Mal sequence with the C275 mutant and with the Pur280-modified form. This shows no variation of the melting temperature for the hairpin but a significant lowering of it for the duplex (see text). The strand concentration was close to  $2 \mu\text{M}$  in all cases.

showed that the melting of the duplex interfering with that of the hairpin for the DIS(Lai) led to a sharpening of the concentration-dependent peak, which was indeed observed (Fig. 5*a*).

**Hairpin-to-Duplex Conversion for the DIS-C275 Mutant**—Subsequently, we analyzed whether the formation of a kissing complex is a prerequisite for the DIS hairpin-duplex transition. For that, we used gel electrophoresis of the DIS-C275 mutant (Fig. 1*a*) unable to form a kissing complex. This RNA was folded at  $20 \mu\text{M}$ , which led to 10% of duplex according to Fig. 3. It was then incubated, either in water at  $37^\circ\text{C}$ , or in presence of salts (20 mM sodium cacodylate, pH 7.0, 25 mM KCl, 2 mM  $\text{MgCl}_2$ ) at 25, 30, or  $37^\circ\text{C}$ , and the fraction of hairpin and duplex was

quantified at various incubation times, which yielded an experimental function as shown in Equation 4,

$$G(t) = \frac{S_D(t)}{S_D(t) + S_H(t)} \approx S_D(t) \quad (\text{Eq. 4})$$

where  $S_D(t)$  and  $S_H(t)$  are the fractions of strands under the duplex and hairpin forms, respectively. The approximation in Equation 1 results from  $S_D(t) + S_H(t) \approx 1$ , because the fraction of melted strand is very small at, or below,  $37^\circ\text{C}$ .

As shown in Fig. 6 and Fig. S1, there is a neat increase of duplex with time at the expense of the hairpin form in the presence of salts, whereas no conversion was observed in water (not shown). As expected, this hairpin-duplex transition is kinetically favored at higher temperatures, with  $\sim 80\%$  of the DIS-C275 strands in the duplex form after 1 day at  $37^\circ\text{C}$ , and around 55 and 45% within 2 days at  $30^\circ\text{C}$  and  $25^\circ\text{C}$ , respectively (the plateaus not being reached; Fig. 6*b*). The concentration dependence agrees with a bimolecular process (Fig. 6*c*). Increasing magnesium concentration from 0.5 mM to 20 mM made duplex formation faster, whereas spermine had a very marginal effect (Fig. 6*d*).

These results show that hairpin-duplex transition does not require a preformed kissing complex. Two mechanisms are therefore possible. The first possibility involves a two-step mechanism: (i) complete melting of the hairpin and (ii) duplex formation from the resulting free single strands. In the second, and only other possibility, no free strand is necessary but, instead, a cruciform intermediate is first generated by the interaction of the ends of two hairpins. This interaction is facilitated by the well known tendency of nucleic acid helices to stack end-to-end as pseudo-continuous helices (as commonly observed in crystals) and by the fraying at the extremities of stems (which is favored at higher temperature). Once formed, the cruciform junction progresses at low energetic cost until its resolution releasing a duplex (Fig. 7*a*). Discrimination between the two possible mechanisms was achieved by the following quantitative kinetic analysis.

The first mechanism is simply described by the two coupled equilibriums.

- (1) Hairpin  $\leftrightarrow$  Strand
- (2) Strand + Strand  $\leftrightarrow$  Duplex

MECHANISM 1

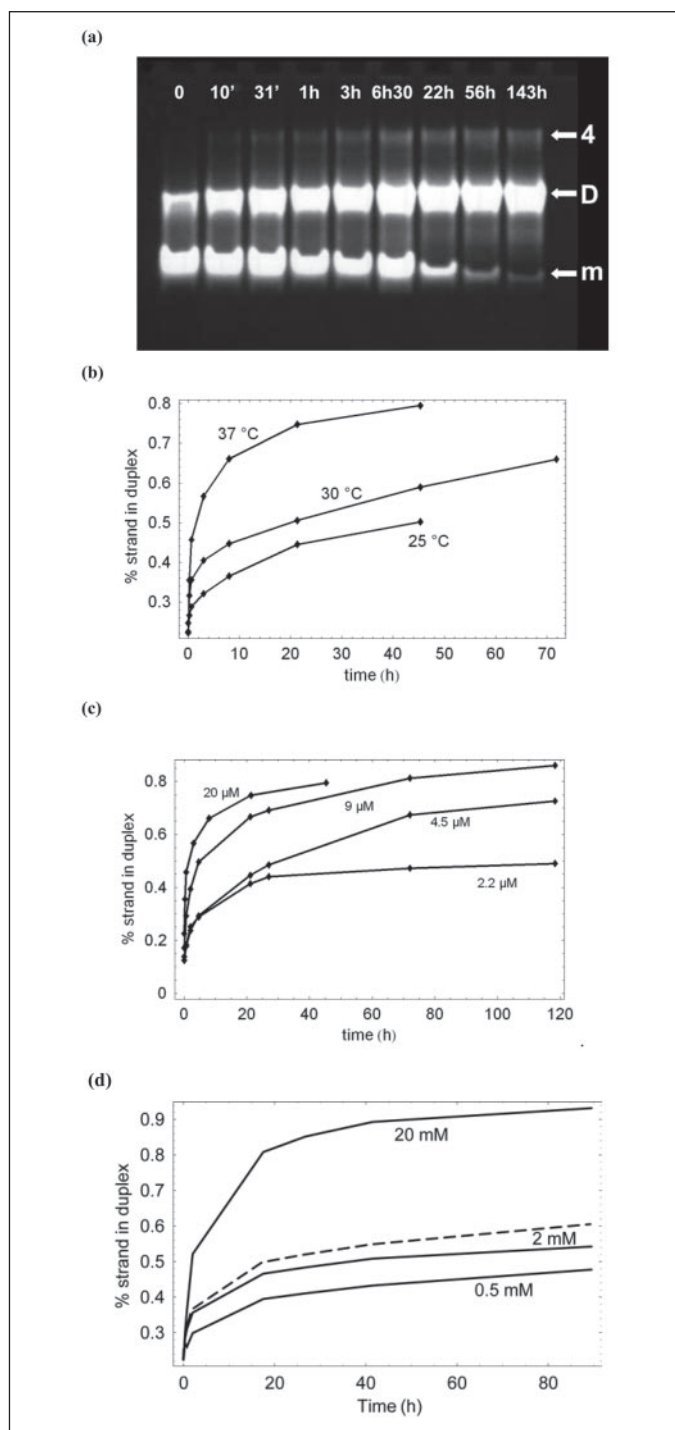


**FIGURE 6. Time-dependent hairpin-duplex transition of the DIS-C275 by incubation with salts (150 mM KCl, 5 mM MgCl<sub>2</sub>, 20 mM sodium cacodylate buffer, pH 6.5) either at different temperatures or with different RNA concentrations.** *a*, gel electrophoresis experiments of the DIS-C275 after incubation at 37 °C during various times. *m* indicates monomer, *D* indicates duplex, and *4* indicates the cruciform intermediate. Note the absence of the cruciform species at *t* = 0 and its increase up to a steady-state concentration after 3 h. *b*, effect of incubation temperature at 20 μM RNA. *c*, effect of RNA concentration with incubation at 37 °C. The results at 2.2 μM RNA are the least reliable because of a very weak staining. *d*, effect of magnesium concentration in absence of spermine for 0.5, 2 (solid curve), and 20 mM. The concentration at 2 mM magnesium is also shown with spermine at 14.6 mM (dashed curve). The RNA concentration was 2.2 μM in all cases. For the sake of comparison, the gels were quantified with ethidium bromide staining for *b* and *c* and with <sup>32</sup>P labeling for *d*.

This yields the following differential and conservation Equations 5–7:

$$\frac{dS}{dt} = k_1H - k_{-1}S \quad (\text{Eq. 5})$$

$$\frac{dD}{dt} = k_2C_{\text{tot}}S^2 - k_{-2}D \quad (\text{Eq. 6})$$

$$S + H + 2D = 1 \quad (\text{Eq. 7})$$

where  $C_{\text{tot}}$  is the total concentration in strand, and  $S$ ,  $H$ , and  $D$  correspond to the reduced concentrations (*i.e.* divided by  $C_{\text{tot}}$ ) of single strand, hairpin, and duplex species, respectively. The situation is favorable because the kinetic constants for hairpin and duplex formation are reasonably known (see “Materials and Methods”). Because the relaxation time for hairpin opening/closing (in Mechanism 1, “(1)”) is much smaller than that for the bimolecular process of duplex formation (in Mechanism 1, “(2)”),  $H$  and  $S$  are always very close to equilibrium, that is  $S \approx K_1H$ , with  $K_1 = (k_1/k_{-1})$ . This results in the following single differential Equation 8,

$$\frac{dD}{d\theta} = D^2 - (1 + k_{-2}\tau)D + \frac{1}{4} \quad (\text{Eq. 8})$$

with  $\theta$  a reduced time  $t/\tau$  with the characteristic time  $\tau$  equal to (Equation 9),

$$\tau = \frac{(1 + K_1)^2}{4k_2C_{\text{tot}}K_1^2} \approx \frac{1}{4k_2C_{\text{tot}}K_1^2} \quad (\text{Eq. 9})$$

the approximation in Equation 9 being justified by  $K_1 \ll 1$  (at most,  $K_1 \approx 3.5 \times 10^{-4}$ ) because the maximum temperature in use (37 °C) is well below the hairpin melting temperature (72 °C).

Equation 8 would easily be integrated, but it is sufficient for our purpose to compare the values at different temperatures of the initial slopes (Equation 10)

$$\left. \frac{dD}{dt} \right|_{t=0} = \frac{1}{\tau} \left. \frac{dD}{d\theta} \right|_{\theta=0} \quad (\text{Eq. 10})$$

from this model with those experimentally observed from  $G(t)$  as defined by Equation 4. One has the simple link shown in Equation 11,

$$\left. \frac{dG}{dt} \right|_{t=0} \approx 2 \left. \frac{dD}{dt} \right|_{t=0} \quad (\text{Eq. 11})$$

because there are two strands per duplex. From the preceding it may easily be obtained as shown in Equation 12,

$$\left. \frac{dG}{dt} \right|_{t=0} \approx 2C_{\text{tot}}H_0^2K_1^2k_2 \left( 1 - \frac{D_0\tilde{H}^2}{H_0^2\tilde{D}} \right) \quad (\text{Eq. 12})$$

with  $H_0$  and  $D_0$  corresponding to the fractions of hairpin and duplex forms at  $t = 0$ , and  $\tilde{H}$  and  $\tilde{D}$  to their values at thermodynamic equilibrium (the ratio  $\tilde{D}/\tilde{H}^2$  is thus equal to  $K_1^2K_2C_{\text{tot}}$ , with  $K_1^2K_2$  the equilibrium constant of the overall process hairpin + hairpin  $\leftrightarrow$  duplex). Again, the approximation in Equation 12 results from  $K_1 \ll 1$ . The product  $2C_{\text{tot}}H_0^2K_1^2k_2$  in Equation 12, which may be expressed as Equation 13,

$$2C_{\text{tot}}H_0^2e^{\frac{\Delta H_1}{RT}m_1}e^{-\frac{2\Delta H_1 + E_{d2}}{RT}} \quad (\text{Eq. 13})$$

## Hairpin-Duplex Conversion

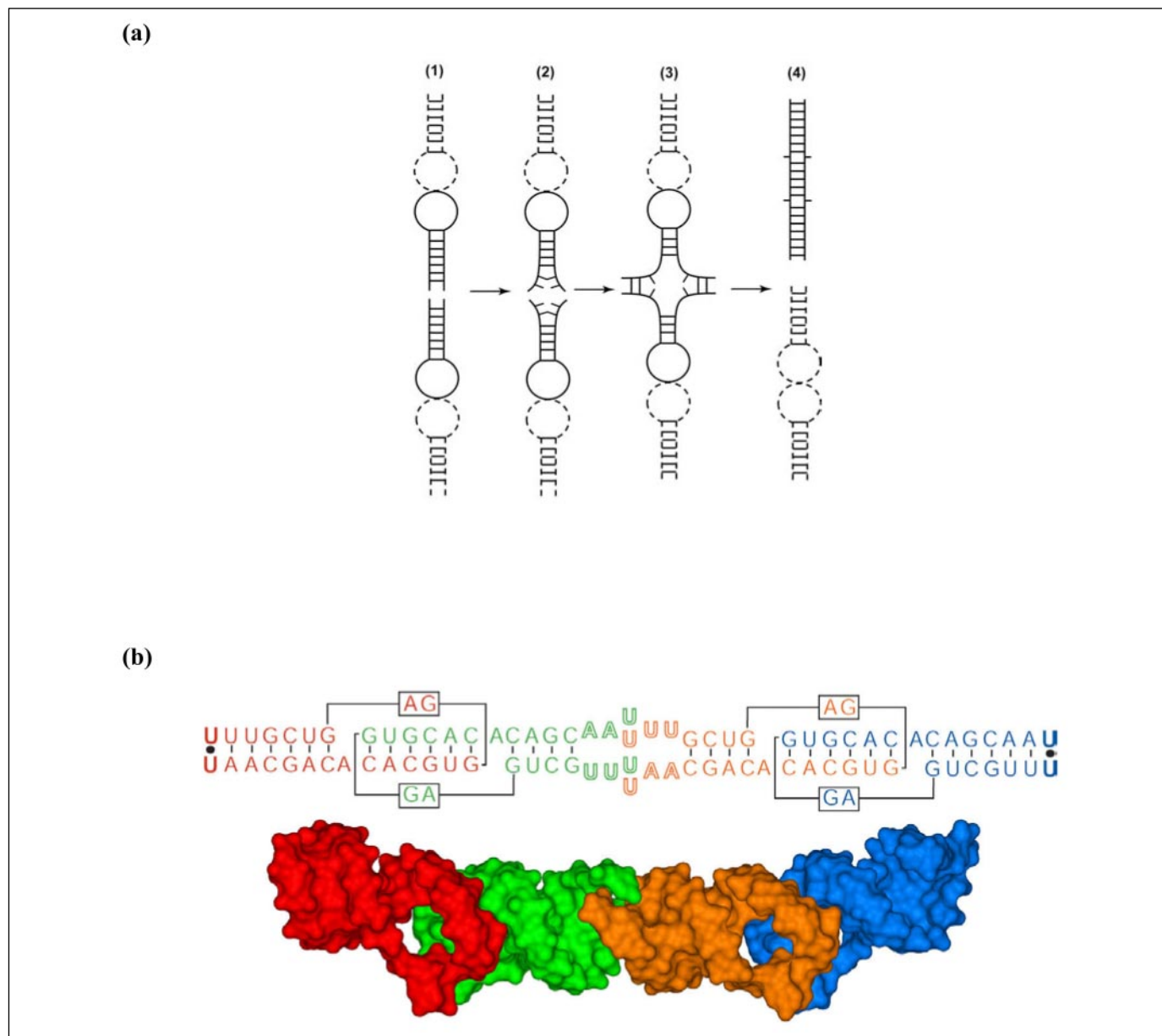


FIGURE 7. *a*, possible hairpin-duplex transition mechanism via cruciform intermediates. The process initiates by the stacking of two hairpins (*step 1*), fraying at both ends (*step 2*), and breaking of terminal intramolecular base pairs that are subsequently reformed as equivalent intermolecular base pairs, forming a cruciform intermediate (*step 3*). The latter is resolved by progression of the junction at low energy cost, releasing a duplex (*step 4*). The figure emphasizes that the same mechanism also applies to the interaction of hairpins engaged in kissing complex (*dashed lines*). In such a case, two hairpin loops are also released and are shown here after reformation of a kissing-complex. *b*, two-dimensional representation of step 2 and three-dimensional structure representative of it, as observed in the kissing-loop complex crystals of the DIS(Mal)UU (Protein Data Bank code 1K9W). The color coding is identical in the two figures. This experimental observation of step 2 was possible because of the presence of a U-U mismatch at the end of the stem, which favored fraying; otherwise, step 1 is commonly observed in crystals of nucleic acids helices.

involves  $(2\Delta H_1 + E_{a2}) \approx 100 \text{ kcal}\cdot\text{mol}^{-1}$  in the exponential term varying with temperature. Therefore, the temperature dependence of this product is much more pronounced than that of  $\bar{D}/F^2 = K_1^2 K_2 C_{\text{tot}}$  in parentheses, which involves  $(2\Delta H_1 + \Delta H_2) \approx -50 \text{ kcal}\cdot\text{mol}^{-1}$  in the exponential term varying with temperature ( $\Delta H_2) \approx -150 \text{ kcal}\cdot\text{mol}^{-1}$  to explain the duplex-to-hairpin ratio observed at equilibrium for  $37^\circ\text{C}$  and for  $20 \mu\text{M}$  in strands (Fig. 6*b*). This implies that the ratio of  $dG/dt_{t=0}$  at two temperatures  $T_1$  and  $T_2$ , and the same  $C_{\text{tot}}$  and  $H_0$ , is very close to Equation 14,

$$\rho = \frac{G'(t=0, T=T_1)}{G'(t=0, T=T_2)} \approx e^{-\frac{2\Delta H_1 + E_{a2}}{R} \left( \frac{1}{T_1} - \frac{1}{T_2} \right)} \quad (\text{Eq. 14})$$

which was confirmed by numerical calculations.

For  $T_1 = 37^\circ\text{C}$  and  $E_{a2} = -5 \text{ kcal}\cdot\text{mol}^{-1}$ , Equation 14 yields  $\rho \approx 560$  for  $T_2 = 25^\circ\text{C}$  and  $\rho \approx 38$  for  $T_2 = 30^\circ\text{C}$ , whereas the observed values with the data for Fig. 6*b* are  $\rho \approx 3$  and  $\rho \approx 1.9$ , respectively. Such low values can be explained by Equation 14, but only by replacing the actual value of  $2\Delta H_1$  by a much smaller value ( $22 \text{ kcal}\cdot\text{mol}^{-1}$ ). This is consistent with a mechanism requiring only a partial melting of the hairpin to initiate the transition to the duplex form. Our experimental data thus imply that a cruciform intermediate has to be formed. Notably, the present conclusion does not depend on whether or not a kissing complex can be formed; it only depends on the disagreement with observations of the hypothesis that hairpins would have to melt fully to allow duplex formation.

This result is contradictory with the one obtained in Ref. 34 with two DIS-like oligonucleotides L1 and L2 able to form a heteroduplex L1-L2. It was concluded that the transition to duplex was strongly dependent on the ability of forming a kissing complex between L1 and L2 and that this transition proceeded through complete hairpin melting. However, we note that the values of the kinetic constants for duplex formation that were obtained at 37, 40, 45, 50, and 55 °C (Fig. 6*a* in (34)) agree well with an activation energy of 31 kcal·mol<sup>-1</sup>. Such a low value is even inconsistent with the melting of only the upper part of the hairpin stems in L1 and L2 (8 bps comprising six G-C). Also, it was noticed in Ref. 34 that the kinetics of duplex formation was not significantly affected by shortening from 8 to 6 bps the upper part of the stems in L1 and L2 hairpins. We point out that this is also consistent with the fact that the whole hairpin stem does not influence the activation energy of the transition. A sequence L1A, with six As being substituted for the nine nucleotide DIS(Lai) apical loop present in L1, showed no duplex formation after 5 h. This was attributed to the complete loss of kissing complex formation between L1A and L2. However, this is a purely kinetic argument. Instead, one may invoke that replacing six consecutive G-C base pairs in the L1-L2 duplex by six mismatches in L1A-L2, which in turn forces three more residues in L2 to form an internal loop, also induces a strong destabilization of the duplex itself. This is a thermodynamic argument valid for any path from hairpin to duplex. It thus appears that the data in Ref. 34 (at least, those for the leadzyme systems that were reported at different temperatures) may be reconciled with a transition from hairpins to duplex involving a cruciform intermediate. This also agrees with the strong acceleration of duplex formation that was observed with the NCp7 that has a well known chaperone-like activity (35–37).

In the present case, the conclusion that a cruciform intermediate is formed *en route* to duplex formation is further supported by two observations. First, we observed slowly migrating species on gels that were not present at the beginning of the experiment and that could correspond to several states of the cruciform intermediate (Fig. 6*a* and Fig. S2). This is in agreement with the well known slow migration of cruciform species (38). Second, the monoclinic DIS kissing complex crystal structure (20), obtained with a mutant sequence where the first G-C base pair of the stem was replaced by a destabilizing U-U mismatch (DIS-UU, Fig. 1*a*), showed hairpins engaged in an interaction strikingly representative of the initial step of cruciform-intermediate formation (Fig. 7*b*). Such a hairpin-duplex conversion through formation of cruciform intermediates has already been invoked several times for DNA (30, 39–42). This also has been mentioned as a possibility for a 24-mer RNA hairpin (43).

## DISCUSSION

Our results on the DIS(Mal) and DIS(Lai) with molecular beacons, as well as on the DIS-C275 mutant on gels, do not fit with the common perception of a crucial and systematic importance of the cooling procedure on the hairpin/duplex ratio. Indeed, many structural studies relied on a flash cooling procedure to ensure the formation of the hairpin form. This was the case for several crystallographic studies (see Introduction) as well as for an NMR study of the DIS(Lai) kissing complex (44). More importantly, most of the crystal studies performed for describing a hairpin structure finally resulted in the description of a duplex structure, which clearly shows that the cooling procedure was unimportant. This is also well illustrated by the first crystal structure of an isolated hairpin obtained after a slow cooling procedure (11, 12). For the NMR DIS(Lai) kissing complex structure, an ultra-fast cooling procedure of a 30 μM RNA sample was reported to yield the hairpin form

(44). Our own observations demonstrated a majority of the duplex after such a treatment. The only difference with the sequence that we used comes from the displacement of two G-C base pairs in the stem. It seems unlikely that such a small change had important consequences on the folding kinetics. In addition, we have observed that upon addition of buffer there was a significant fluorescence increase (Fig. S3), which can only be interpreted as an additional increase of the duplex form. One may therefore raise questions about the relevance of the distorted structure in Ref. 44, with helices far from the standard A-form geometry.

In retrospect, our results are in good agreement with several observations. First, Takahashi *et al.* (45) observed that the DIS(Lai) 23-mer mainly formed duplex at 20 μM, even after flash cooling. Second, another study involving hairpins with various loop sequences showed that the hairpin/duplex ratio after ultra-fast or slow cooling was strongly dependent on the self-complementarity of the loop (27). These results can be directly compared with ours, also obtained by gel electrophoresis (Fig. 4). From both studies, it can be seen that for a given hairpin sequence, the amount of duplex species resulting from annealing is essentially dependent on the self-complementarity in the loop. The two wild-type DIS with a six-residue self-complementary sequence very easily forms duplex, whereas the DIS-C275 mutant remains in hairpin form at higher concentrations. Also, the ΔC56 hairpin used by Kirchner *et al.* (27), with a nonself-complementary sequence, remains in the hairpin form even at millimolar concentrations. Hairpins ΔA58 and ΔU59 are intermediate species, and their duplex-forming propensity can also be ranked according to the same criterion: ΔA58 with two self-complementary residues in the loop yields the hairpin form at higher concentration than ΔU59 with four self-complementary residues in the loop.

As already discussed previously, these results can apparently be rationalized in two ways. First, the yield increase in the hairpin form may be obviously because of the lack of a self-complementary sequence, which destabilizes the duplex but not the hairpin. Second, as invoked in Refs. 27 and 34, the lack of this self-complementary loop sequence, by preventing kissing complex formation, would also suppress a necessary intermediate prior to duplex formation. Again, the first argument is thermodynamic, whereas the second one points only to the kinetics of transition. Indeed, there exists some kinetic effects; ΔA58 in Fig. 4 shows some dependence with the kinetics of cooling. However, the effect is rather small and it is nonexistent for our DIS-related sequences. In fact, a thorough understanding of such quick annealing experiments requires the integration of the differential equations (as Equations 5 and 6) governing the kinetics of interconversion between the different species. We have performed a general theoretical study, as well as numerical investigations in many different cases. This will be developed further elsewhere.<sup>5</sup> The major theoretical result is that there exists well defined thresholds in temperature where the concentrations of different species reach their equilibrium values upon heating, or depart from them upon cooling. An important finding is that such threshold temperatures, separating equilibrium from nonequilibrium regimes, have a logarithmic dependence with the rate of heating or cooling and thus have little dependence on it. This is consistent with our observations on the annealing of the DIS(Mal) and DIS(Lai) sequences. Such unexpected behavior suggests that the outcome of annealing experiments does not depend only on whether or not a kissing complex can be formed. Rather, it appears that there is a complex interplay between the threshold temperature and the equilibrium concentrations reached at this temperature during the cooling process.

Our previous crystallization results are in good agreement with the present fluorescence investigations highlighting the importance of RNA concentration during the initial annealing. Previously, we have been

## Hairpin-Duplex Conversion

able to crystallize selectively either the DIS kissing complex (20) or its duplex form (19), depending on the initial RNA concentration used for the folding (routinely 3  $\mu\text{M}$  are used to obtain kissing complex crystals, whereas 60  $\mu\text{M}$  leads to duplex crystals; see "Materials and Methods"). In some cases, a flash cooling protocol led to a kissing complex and duplex crystals in identical MPD-based crystallization conditions with an RNA concentration of about 30  $\mu\text{M}$ .

However, our successful crystallization of the DIS kissing complex, which was incubated during several days at 37 °C in high salt and at high RNA concentration, is contradictory with the hairpin-duplex interconversion observed for the DIS-C275 in presence of salts. This is even more contradictory if one considers that the duplex form of the DIS-C275 mutant is destabilized in comparison of the hairpin form, whereas the duplex with the wild-type sequence is not destabilized. Consequently, the wild-type DIS kissing complex is expected to be converted into duplex even more surely than the DIS-C275, which is obviously not the case because we routinely obtain kissing complex crystals with various sequences. Our interpretation of these apparently inconsistent observations is that for these kissing complex forming sequences, the transition to duplex is blocked by the formation of stable kissing complex dimers interacting through their bulged-out purines, as observed in the crystal packing (20). More importantly, such tetramers of hairpins are considerably favored at high concentrations and, very likely, are formed in solution and constitute the building units of the crystals (which is strongly supported by their systematic occurrence in crystals of kissing complex, whatever the RNA sequence and the crystallization condition). Because the DIS-C275 mutant cannot form a stable kissing complex, it also cannot form tetramers and, accordingly, nothing prevents its complete conversion from hairpin to duplex through a cruciform intermediate. In agreement with our interpretation, Rist and Marino (46) observed in their experimental conditions (25 °C, low salt and low DIS(Mal) concentration) that the initial kissing complex did convert to duplex, but by no more than 25%. This is indeed consistent with our successful crystallization of the kissing complex. This is also consistent with the fact that we observed in one case the coexistence of kissing complex and duplex crystals in the same crystallization drop (Fig. S4).

Many studies have been carried out to investigate the DIS kissing complex to extended duplex transition, either on a similar 23-nucleotide fragment or on larger fragments comprising the complete 39-nucleotide DIS stem-loop (17, 28, 34, 45–52). Notably, the chaperone activity of the NCp7 was shown to facilitate this transition (17). In particular, the internal loop contained in the DIS stem was shown to be required for the formation of the duplex, as the NCp7 protein was unable to convert a DIS kissing complex with this internal bulge replaced by several G-C base pairs (45). Based on experiments performed on the 23-nucleotide fragment, it was also concluded that the formation of the kissing complex was required to form the extended duplex and that the transition was achieved by a rearrangement of the base pairing in stem regions, without disruption of the loop-loop interaction (28, 46). This mechanism deduced from the 23-nucleotide DIS fragment was supposed to explain the observed *in vitro* stabilization of larger HIV-1 genomic RNA fragments.

However, we have shown here, at least for this DIS 23-nucleotide fragment, that the formation of a kissing complex is not a prerequisite for hairpin-to-duplex transition. Our results on a mutated DIS unable to form a kissing complex have shown that the transition can only occur via formation of a cruciform intermediate, progression of the four-way junction until its resolution as a duplex, and definitely not through free single strands generated by hairpin melting. This transition appeared to

be facilitated by a temperature increase, by the presence of salt, and by the self-complementarity of the loop sequence. As it was shown that the NCp7 protein enhances fraying at stem extremities of nucleic acid hairpins (37), this protein may be viewed as mimicking a temperature increase. It thus may be proposed that it also promotes duplex formation by the formation of a cruciform junction. This destabilizing activity is likely facilitated by the presence of the internal loop of the DIS stem, as already suggested (48).

It is unlikely that the transition we observed on the 23-nucleotide RNA fragment is relevant for the putative *in vivo* DIS hairpin-duplex transition. The main reasons are as follows: first that *in vivo* the DIS stem-loop is embedded within the very structured 5'-untranslated region, and second that such a mechanism would require two interacting kissing complexes (as shown in Fig. 7a). However, such a hairpin-duplex transition with cruciform intermediates might be more relevant to the first strand transfer where the minus "strong-stop" DNA is translocated to the 3'-end of the genomic RNA. This requires the annealing of the *trans*-activation response element (TAR), a stem loop localized at both ends of the HIV-1 genome, to its neo-synthesized complementary sequence cTAR. This reaction requires a destabilization of the very stable TAR and cTAR stem-loops. Because it has been shown that NCp7 enhances the melting of TAR and cTAR by promoting fraying on the stem termini (37), it may be proposed that their hybridization could be achieved via formation of a cruciform intermediate, alternatively to prior formation of a TAR-cTAR kissing complex further stabilized into a full duplex.

It is also noticeable that the size of the RNA we have studied is comparable with that of the so-called  $\mu\text{RNAs}$  and small interfering RNAs that have been shown to play important regulatory roles (53). It has also been demonstrated that there exists a sequence bias for a weaker stability at one end of these regulatory RNAs (54). It may thus be considered that a helicase might not always be necessary to promote hairpin-duplex transition *in vivo*. Our results show that such a transition is rather fast at 37 °C (at 20  $\mu\text{M}$  in strands) in rather low saline conditions (Fig. 6c). By its temperature dependence, this might also be at the basis of a "thermosensor" comparable with those known to regulate gene expression at the post-transcriptional level (55).

---

*Acknowledgments*—We are grateful to Bernard and Chantal Ehresmann for their constant support. We thank P. Wolff for help in RNA purification. We are grateful to the referee for an important and constructive comment about our original manuscript.

---

*Note Added in Proof*—After submission of this paper, another work (Liu, H-W., Landes, C. F., Zeng, Y., Kovaleski, B. J., Muller, D. G., Barany, G., Musier-Forsyth, K., and Barbara, P. F. (2005) *Biophys. J.*, in press) also mentioned the cruciform pathway as a possibility for TAR-cTAR annealing.

## REFERENCES

1. Aboul-ela, F., Nikonowicz, E. P., and Pardi, A. (1994) *FEBS Lett.* **347**, 261–264
2. Cabello-Villegas, J., and Nikonowicz, E. P. (2000) *Nucleic Acids Res.* **28**, e74
3. Jovine, L., Hainzl, T., Oubridge, C., Scott, W. G., Li, J., Sixma, T. K., Wonacott, A., Skarzynski, T., and Nagai, K. (2000) *Struct. Fold. Des.* **8**, 527–540
4. Wild, K., Weichenrieder, O., Leonard, G. A., and Cusack, S. (1999) *Struct. Fold. Des.* **7**, 1345–1352
5. Shah, S. A., and Brunger, A. T. (1999) *J. Mol. Biol.* **285**, 1577–1588
6. Klosterman, P. S., Shah, S. A., and Steitz, T. A. (1999) *Biochemistry* **38**, 14784–14792
7. Ennifar, E., Nikulin, A., Tishchenko, S., Serganov, A., Nevskaya, N., Garber, M., Ehresmann, B., Ehresmann, C., Nikonov, S., and Dumas, P. (2000) *J. Mol. Biol.* **304**, 35–42, and references therein
8. Oubridge, C., Ito, N., Evans, P. R., Teo, C. H., and Nagai, K. (1994) *Nature* **372**, 432–438
9. Wild, K., Sinning, I., and Cusack, S. (2001) *Science* **294**, 598–601
10. Tishchenko, S., Nikulin, A., Fomenkova, N., Nevskaya, N., Nikonov, O., Dumas, P.,

- Moine, H., Ehresmann, B., Ehresmann, C., Piendl, W., Lamzin, V., Garber, M., and Nikonov, S. (2001) *J. Mol. Biol.* **311**, 311–324
11. Correll, C. C., Munishkin, A., Chan, Y. L., Ren, Z., Wool, I. G., and Steitz, T. A. (1998) *Proc. Natl. Acad. Sci. U. S. A.* **95**, 13436–13441
  12. Correll, C. C., Wool, I. G., and Munishkin, A. (1999) *J. Mol. Biol.* **292**, 275–287
  13. St. Louis, D. C., Gotte, D., Sanders-Buell, E., Ritchey, D. W., Salminen, M. O., Carr, J. K., and McCutchan, F. E. (1998) *J. Virol.* **72**, 3991–3998
  14. Paillart, J.-C., Berthou, L., Ottmann, M., Darlix, J.-L., Marquet, R., Ehresmann, C., and Ehresmann, B. (1996) *J. Virol.* **70**, 8348–8354
  15. Haddrick, M., Lear, A. L., Cann, A. J., and Heaphy, S. (1996) *J. Mol. Biol.* **259**, 58–68
  16. Paillart, J.-C., Marquet, R., Skripkin, E., Ehresmann, C., and Ehresmann, B. (1996) *Biochimie (Paris)* **78**, 639–653
  17. Muriaux, D., Rocquigny, H. D., Roques, B. P., and Paoletti, J. (1996) *J. Biol. Chem.* **271**, 33686–33692
  18. Yusupov, M., Walter, P., Marquet, R., Ehresmann, C., Ehresmann, B., and Dumas, P. (1999) *Acta Crystallogr. Sect. D Biol. Crystallogr.* **55**, 281–284
  19. Ennifar, E., Yusupov, M., Walter, P., Marquet, R., Ehresmann, B., Ehresmann, C., and Dumas, P. (1999) *Structure* **7**, 1439–1449
  20. Ennifar, E., Walter, P., Ehresmann, B., Ehresmann, C., and Dumas, P. (2001) *Nat. Struct. Biol.* **8**, 1064–1068
  21. Tyagi, S., and Kramer, F. R. (1996) *Nat. Biotechnol.* **14**, 303–308
  22. Cantor, C. R., and Schimmel, P. R. (1980) *Biophysical Chemistry*, pp. 1109–1264, W. H. Freeman & Co., San Francisco
  23. Turner, D. H. (2000) in *Nucleic Acids, Structure, Properties, and Functions* (Bloomfield, V. A., Crothers, D. M., and Tinocco, L., eds) pp. 259–334, University Science Books, Sausalito, CA
  24. Porschke, D., and Eigen, M. (1971) *J. Mol. Biol.* **62**, 361–381
  25. Craig, M. E., Crothers, D. M., and Doty, P. (1971) *J. Mol. Biol.* **62**, 383–401
  26. Paillart, J. C., Marquet, R., Skripkin, E., Ehresmann, B., and Ehresmann, C. (1994) *J. Biol. Chem.* **269**, 27486–27493
  27. Kirchner, R., Vogtherr, M., Limmer, S., and Sprinzl, M. (1998) *Antisense Nucleic Acid Drug Dev.* **8**, 507–516
  28. Theilleux-Delalande, V., Girard, F., Huynh-Dinh, T., Lancelot, G., and Paoletti, J. (2000) *Eur. J. Biochem.* **267**, 2711–2719
  29. Marky, L. A., Blumenfeld, K. S., Kozlowski, S., and Breslauer, K. J. (1983) *Biopolymers* **22**, 1247–1257
  30. Scheffler, I. E., Elson, E. L., and Baldwin, R. L. (1968) *J. Mol. Biol.* **36**, 291–304
  31. Santa Lucia, J., Jr., Kierzek, R., and Turner, D. H. (1990) *Biochemistry* **29**, 8813–8819
  32. Schroeder, S., Kim, J., and Turner, D. H. (1996) *Biochemistry* **35**, 16105–16109
  33. Longfellow, C. E., Kierzek, R., and Turner, D. H. (1990) *Biochemistry* **29**, 278–285
  34. Windbichler, N., Werner, M., and Schroeder, R. (2003) *Nucleic Acids Res.* **31**, 6419–6427
  35. Tsuchihashi, Z., and Brown, P. O. (1994) *J. Virol.* **68**, 5863–5870
  36. Tsuchihashi, Z., Khosla, M., and Herschlag, D. (1993) *Science* **262**, 99–102
  37. Bernacchi, S., Stoylov, S., Piemont, E., Ficheux, D., Roques, B. P., Darlix, J. L., and Mely, Y. (2002) *J. Mol. Biol.* **317**, 385–399
  38. Yakubovskaya, M. G., Neschastnova, A. A., Humphrey, K. E., Babon, J. J., Popenko, V. I., Smith, M. J., Lambrinakos, A., Lipatova, Z. V., Dobrovolskaia, M. A., Cappai, R., Masters, C. L., Belitsky, G. A., and Cotton, R. G. (2001) *Eur. J. Biochem.* **268**, 7–14
  39. Wemmer, D. E., Chou, S. H., Hare, D. R., and Reid, B. R. (1985) *Nucleic Acids Res.* **13**, 3755–3772
  40. Xodo, L. E., Manzini, G., Quadrifoglio, F., Yathindra, N., van der Marel, G. A., and van Boom, J. H. (1989) *J. Mol. Biol.* **205**, 777–781
  41. Avizonis, D. Z., and Kearns, D. R. (1995) *Biopolymers* **35**, 187–200
  42. Hald, M., Pedersen, J. B., Stein, P. C., Kirpekar, F., and Jacobsen, J. P. (1995) *Nucleic Acids Res.* **23**, 4576–4582
  43. Borer, P. N., Lin, Y., Wang, S., Roggenbuck, M. W., Gott, J. M., Uhlenbeck, O. C., and Pelczar, I. (1995) *Biochemistry* **34**, 6488–6503
  44. Mujeeb, A., Clever, J. L., Billeci, T. M., James, T. L., and Parslow, T. G. (1998) *Nat. Struct. Biol.* **5**, 432–436
  45. Takahashi, K. I., Baba, S., Chattopadhyay, P., Koyanagi, Y., Yamamoto, N., Takaku, H., and Kawai, G. (2000) *RNA (N. Y.)* **6**, 96–102
  46. Rist, M. J., and Marino, J. P. (2002) *Biochemistry* **41**, 14762–14770
  47. Muriaux, D., Fossé, P., and Paoletti, J. (1996) *Biochemistry* **35**, 5075–5082
  48. Takahashi, K., Baba, S., Hayashi, Y., Koyanagi, Y., Yamamoto, N., Takaku, H., and Kawai, G. (2000) *J. Biochem. (Tokyo)* **127**, 681–686
  49. Takahashi, K. I., Baba, S., Koyanagi, Y., Yamamoto, N., Takaku, H., and Kawai, G. (2001) *J. Biol. Chem.* **276**, 31274–31278
  50. Baba, S., Takahashi, K., Nomura, Y., Noguchi, S., Koyanagi, Y., Yamamoto, N., Takaku, H., and Kawai, G. (2001) *Nucleic Acids Res., Suppl.* **1**, 155–156
  51. Baba, S., Takahashi, K., Koyanagi, Y., Yamamoto, N., Takaku, H., Gorelick, R. J., and Kawai, G. (2003) *J. Biochem. (Tokyo)* **134**, 637–639
  52. Mihalescu, M. R., and Marino, J. P. (2004) *Proc. Natl. Acad. Sci. U. S. A.* **101**, 1189–1194
  53. Bartel, D. P. (2004) *Cell* **116**, 281–297
  54. Khvorova, A., Reynolds, A., and Jayasena, S. D. (2003) *Cell* **115**, 209–216
  55. Narberhaus, F. (2002) *Arch. Microbiol.* **178**, 404–410